Proceedings of the 17th World Congress
The International Federation of Automatic Control
Seoul, Korea, July 6-11, 2008

Optimizing Control of Hot Blast Stoves in Staggered Parallel Operation

Akın Şahin and Manfred Morari

Automatic Control Laboratory, ETH Zurich, 8092 Zurich, Switzerland
(e-mail: sahin, morari@control.ee.ethz.ch)

Abstract: An optimizing control scheme is designed for the minimization of the energy consumption in the hot blast stoves. By an appropriate selection of the control structure, the problem of energy minimization at steady-state in the presence of constraints is formulated as a constrained optimal control problem. A model predictive control (MPC) scheme is designed based on a simple linear control model, which is obtained from step response experiments on a detailed dynamical model of the process. The control model is augmented with an integrating disturbance model to compensate the steady-state offset. The performance of the MPC scheme is tested on the detailed dynamical model.

Keywords: Advanced process control, Optimal control, Model predictive control

1. INTRODUCTION

The efficient operation of the blast furnace requires the maintenance of the hot blast at a certain flow rate and temperature. The hot blast is supplied to the furnace by hot blast stoves. A hot blast stove is a tall, cylindrical thermal regenerator comprising a large mass of solid material called checkerwork, as shown in Fig. 1. The checkerwork is composed of several refractory brick layers and contains many flues, where the gas flows through. A hot blast stove goes through the alternate cycles of heating and cooling, named as *on-gas phase* and *on-blast phase* respectively. During the on-gas phase the hot gas arising from the combustion process flows through the checkerwork and heats the refractory brick. During the on-blast phase the cold blast with a lower entrance temperature flows through the hot checkerwork in the reverse direction, it is heated up and fed into the blast furnace. The staggered

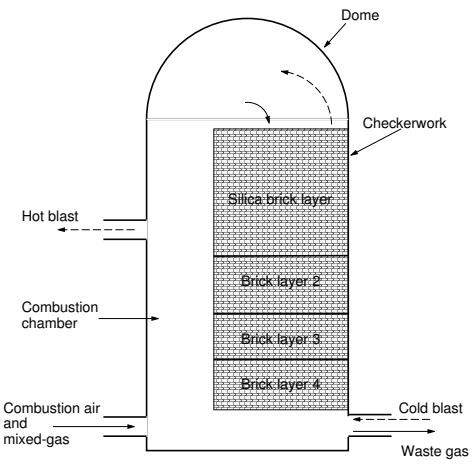

Fig. 1. Hot blast stove

parallel operation, depicted in Fig. 2, is an arrangement of four hot blast stoves. In this arrangement, while two stoves are heated up, the other two stoves supply the hot blast simultaneously. These two hot blast streams are mixed together with the cold blast to supply the blast furnace with hot blast at the desired temperature and flow rate.

The energy consumption of the operation is determined by the heat supply during the on-gas phase, which is determined by the amount of fuel used during the combustion process. It is the purpose of this study to minimize the heat supply to the stoves while supplying the blast furnace with hot blast at the required temperature and flow rate. Initial studies concerning the optimal operation of hot blast stoves in staggered parallel operation started with the work of Kwakernaak et al. [1970]. In this work they investigated the optimal operation of a single stove under stationary periodic operation, i.e. the load, which is defined as the reference blast temperature and flow rate, does not change. Zuidema [1970] extended this work by analyzing the operation under load changes. The single stove operation of hot blast stoves has also received attention. Matoba et al. [1986] developed an optimal regulator based on a linear model. Muske [2000] developed a nonlinear model-based predictive control scheme to minimize the heat input to the stoves.

In this work we study optimizing the staggered parallel operation of the hot blast stoves with no load changes. We consider the on-gas and on-blast phase durations as fixed, which is commonly done in industry. Since the economics is primarily determined by the steady-state performance, we are concerned with optimizing the operation at steady-state. The appropriate selection of the controller structure with the corresponding controlled variables and the sampling time and including the constraints in the problem formulation allows us to formulate the steady-state optimizing control of hot blast stoves as a constrained optimal control problem. We use model predictive control (MPC) for solving the constrained optimal control problem.

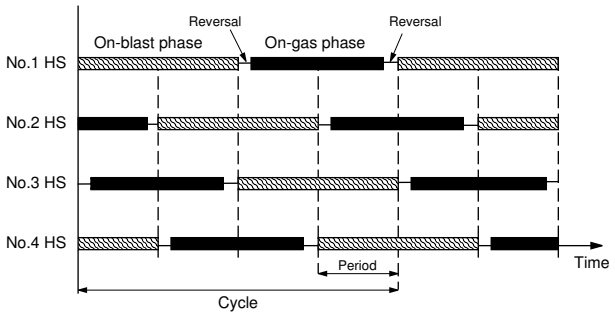

Fig. 2. Staggered parallel operation of hot blast stoves

2. PROCESS DESCRIPTION

The staggered parallel operation is depicted in Fig. 2. As may be seen in this figure, the operation of each stove is switched periodically between the on-gas and on-blast phases, which have constant durations. Moreover, the operation of each stove is shifted in time with respect to the other stoves. Defining *cycle* as the duration from the start of an on-gas phase to the end of the following on-blast phase, the operation of the stoves are repeated at every cycle. Therefore, the staggered parallel operation of the four stoves can be characterized as a time-varying periodic system. On the other hand, in the controller synthesis by sampling the continuous operation of the stoves only at every cycle we consider the process as a time-invariant system. In other words, for designing the controller we translate the time-varying periodic dynamics of the system into time-invariant dynamics. The details of this sampling are given later while explaining the control models. It is important to note that while the steady-state for the staggered parallel operation is a cyclic steady-state, it is constant for the control system. For the rest of the paper we will not distinguish between these two terms and simply use the term *steady-state*.

During the on-gas phase combustion air enriched with the coke oven gas burns in the combustion chamber and produces the high temperature exhaust gas, which flows through the checkerwork and heats it up. In this work we assume that the ratio of the combustion air/coke oven gas is fixed, which results in a constant exhaust gas temperature entering the stove. Therefore, the amount of heat entering the stove during the on-gas phase is determined only by the exhaust gas flow rate. In this work, the exhaust gas flow rate is assumed to have a constant pattern throughout the on-gas phase.

In the on-blast phase the two hot blast streams coming from the on-blast phase stoves and the cold blast, which is not fed through the stoves, are mixed in order to obtain the desired blast temperature and flow rate. The mixing policy used in this work is depicted in Fig. 3. Since the exit blast temperature decreases with time, the stove that just starts its on-blast phase has a relatively high blast temperature. The blast with high temperature is employed only after the blast temperature of the other stove becomes lower than the reference blast temperature. During the period, where only one stove supplies hot blast, the reference blast temperature is maintained by mixing cold blast. Due to safety reasons, there is a lower limit on the minimum amount of the cold blast mixing flow rate. In the period where both stoves supply hot blast the cold blast mixing volume is kept at this minimum value.

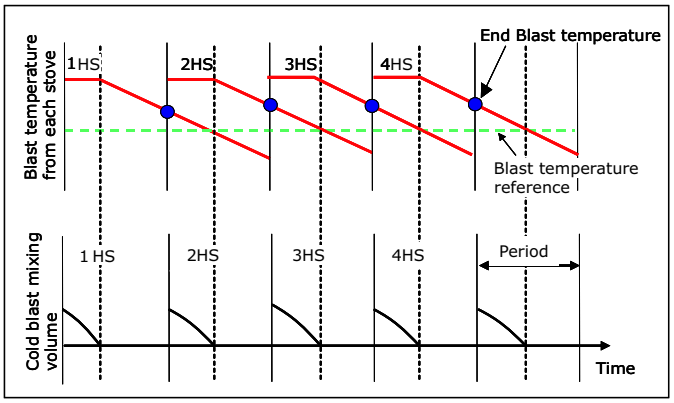

Fig. 3. Schematic explanation of the on-blast phase mixing policy

3. PROBLEM FORMULATION

3.1 Degrees of freedom for control and constraints

During the on-blast phase local controllers adjust the flow rates of the two hot blast streams and the cold blast stream to obtain the required temperature of the mixed stream, the hot blast entering the blast furnace. Hence, there is no degree of freedom for optimization during the on-blast phase. As mentioned in the process description, the amount of heat produced during the combustion process is only a function of the exhaust gas flow rate. Therefore, the only degree of freedom for control in the staggered parallel operation is the exhaust gas flow rate.

Two most critical constraints are considered in this work. The first constraint is the lower bound on the cold blast mixing volume as it was explained in the process description. The other critical constraint we consider in this work is the minimum silica brick temperature constraint. The brick temperature at the bottom of the silica brick layer, shown in Fig. 1 must be kept above a lower bound. Since the stove temperature is minimum at the end of the on-blast phase, the silica brick temperature is evaluated only at that time instant.

3.2 Optimal operation and controlled variable selection

The aim of this work is to minimize the heat input to the stoves and since the economic performance is primarily determined by steady-state considerations, we are mainly concerned with optimizing the operation at steady-state.

To design a control scheme we first need to identify the controlled variables, which are indicative of the excessive heat supply to the plant. The set points for these controlled variables should define the optimal operation point. To identify these controlled variables we first study the behavior of the plant when excessive heat input is supplied.

Let's assume the system is initially at the optimal operating point with the minimal heat supply. When the heat supply increases some of the excess heat input will

be accumulated in the stove until the next steady-state operating point is reached. The temperature profile of the stove increases due to the accumulated heat. When the temperature along the stove increases, the blast temperature leaving the stove during the on-blast phase also increases. In order to obtain the reference temperature more cold blast should be mixed. Therefore, the amount of cold blast mixing volume used in the on-blast phase is an indicator of the excessive heat input. By minimizing the cold blast mixing volume we can minimize the excessive heat supply. However, since cold blast mixing flow rate is a time-varying variable, it is hard to assign a set point for it. Instead we use the end blast temperature as the controlled variable, which is a direct measure of the cold blast mixing flow rate as may be seen in Fig. 3. The cold blast mixing peak at the start of the period is determined by the end blast temperature of the stove which supplies the blast to the furnace together with the cold blast mixing. The lower the end blast temperature, the lower the peak cold blast mixing flow. However, the peak flow rate at the start of a period cannot be lower than the lower bound. In order to avoid the cold blast flow rate dropping below this lower bound in case of external disturbances, operators would keep a certain peak value well above the lower bound. The end blast temperature providing this peak value can be determined from the operational data and assigned as the constraint of the end blast temperature.

3.3 Control problem

In summary, the control problem is to develop a constrained optimal control scheme that drives down the end blast temperature to its constraint by manipulating the exhaust gas flow rate while respecting the brick temperature constraint.

4. MODELING

4.1 Heat transfer mechanism in a single stove

While modeling the heat transfer mechanism within the stoves the following commonly accepted assumptions are made (Kwakernaak et al. [1970],Matoba et al. [1986]): a) Heat losses to the environment are ignored; b) Axial and radial heat conductions in the brick are ignored; c) Heat capacity of the gas or blast is negligibly small relative to the heat capacity of the checkerwork; d) Heat transfer occurring at the reversals is neglected.

Based on these assumptions, the heat transfer can be described by the following partial differential equations (Kwakernaak et al. [1970]):

$$\frac{\partial T_g(t,y)}{\partial y} = -\frac{ha}{c_g V(t) l}\left[T_g(t,y) - T_s(t,y)\right] \quad (1)$$

$$\frac{\partial T_s(t,y)}{\partial t} = \frac{ha}{m c_s}\left[T_g(t,y) - T_s(t,y)\right] \quad (2)$$

T_g	gas temperature [$^\circ$C]
T_s	solid temperature [$^\circ$C]
t	time [min]
y	vertical distance [m]
h	overall heat transfer coefficient (convection and radiation) [$\mathrm{J^\circ C^{-1}min^{-1}m^{-2}}$]
a	chequerwork heating surface area [$\mathrm{m^2}$]
V	gas flow rate [$\mathrm{kgmin^{-1}}$]
c_g	specific heat of gas [$\mathrm{J^\circ C^{-1}kg^{-1}}$]
l	height of the chequerwork [m]
m	mass of the chequerwork [kg]
c_s	specific heat of chequerwork [$\mathrm{J^\circ C^{-1}kg^{-1}}$]

In equations (1) and (2) c_s and c_g are temperature dependent and h is both temperature and flow rate dependent. The boundary conditions for the partial differential equations are given by the entrance gas temperatures. The temperature of exhaust gas entering the stove during the on-gas phase and cold blast entering the stove during the on-blast phase are constant. The initial temperature profile of the stove at the beginning of a phase is given by the terminal stove temperature profile of the preceding phase.

We will not mention the method of solving the partial differential equations given in (1) and (2) here. Willmott [1964] presents a detailed solution in his work, where the basic idea is to discretize the system in both spatial and time dimensions.

4.2 Modeling the staggered parallel operation

In staggered parallel operation each stove is modeled with the heat transfer mechanism described by the partial differential equations (1) and (2). All the stoves are assumed to have same dynamics, i.e., they have the same parameters. The reversal periods between periods between the two phases are ignored. The on-blast phase mixing policy described previously is implemented in the model. The flow rates of the hot blast streams and the cold blast mixing are calculated based on the mass and energy balance equations, details of which will not be given here due to limited space.

5. CONTROL CONCEPT

In order to solve the constrained optimal control problem we formulated we used Model Predictive Control (MPC). MPC has proven to be a powerful control technique in the process industry due to its ability to handle multivariable systems and incorporate constraints in the problem formulation, (Maciejowski [2002]). In MPC an internal model is used to predict the future evolution of the plant. An optimal control problem is formulated where the control objectives are formulated in a cost function while the process specifications are expressed as constraints. A sequence of optimal inputs is obtained by solving the optimization problem over a finite horizon. Only the first control move of the sequence is applied on the plant and the optimization procedure is repeated at the next time instant according to a *receding horizon* strategy, which introduces feedback to MPC.

5.1 Control model

In order to predict the future evolution of the plant we have developed a linear time-invariant control model, based on step response experiments on the detailed model. As mentioned before, for controller synthesis we translate time-varying periodic dynamics of the staggered parallel operation into time-invariant dynamics by sampling the system at each cycle. The time elapsed between two successive switching instances is defined as *period*, as shown in Fig. 2. Assuming on-gas and on-blast phases have equal durations, each cycle lasts for four periods. During each full cycle the end blast temperature of each stove is measured at the end of the first period of the on-blast phase and brick temperature at the end of the second period of the on-blast phase. Moreover, the exhaust gas flow rate is applied to each stove at the beginning of the first period of its on-gas phase. In summary, within each cycle we measure the 8 output variables and we apply the 4 inputs. Therefore, the staggered parallel operation of hot blast stoves is considered as a time-invariant MIMO system with four inputs, the exhaust gas flow rates $V_g \in \mathbb{R}^4$, and eight outputs, the end blast temperatures $T_e \in \mathbb{R}^4$ and the brick temperatures $T_b \in \mathbb{R}^4$ of each stove.

The dynamics of the model are approximated around an operating point by doing step response experiments on the detailed model. While the stoves are in a cyclic steady-state at the operating point ($V_{g,0} = 2300\mathrm{Nm}^3/\mathrm{min}$, $T_{e,0} = 1280.5^\circ$, $T_{b,0} = 570^\circ$), a step input of ($\Delta V_g = 5\mathrm{Nm}^3/\mathrm{min}$) is applied to the fourth stove. The deviations of the end blast temperatures from the operating point per step input, $\Delta T_e/\Delta V_g$ are shown in Fig. 4. Since all the stoves have the same dynamics, similar step responses are obtained when a step input is applied to the other input channels. As may be seen in Fig. 4 the deviation of each output variable from the operating point per unit step input can be approximated by a first order linear system. A very similar step response with different steady-state gains applies for the brick temperature and the deviations of the brick temperatures can also be approximated by first order linear systems. As a result we obtain the following linear discrete-time model:

$$x(k+1) = Ax(k) + Bu(k) \tag{3}$$

$$y(k) = Cx(k) \tag{4}$$

with

$$x = \begin{bmatrix} x_e \\ x_b \end{bmatrix},\ y = \begin{bmatrix} y_e \\ y_b \end{bmatrix}, \tag{5}$$

$$A = \begin{bmatrix} A_e & 0 \\ 0 & A_b \end{bmatrix},\ B = \begin{bmatrix} B_e \\ B_b \end{bmatrix},\ C = \begin{bmatrix} C_e & 0 \\ 0 & C_b \end{bmatrix}. \tag{6}$$

In the above equations the subscript "e" denotes the variables related to the end blast temperature and the subscript "b" is for brick temperature. $x_e, x_b \in \mathbb{R}^4$ are the states, $u \in \mathbb{R}^4$ and $y_e, y_b \in \mathbb{R}^4$ are the deviations of input and output from the operating point.

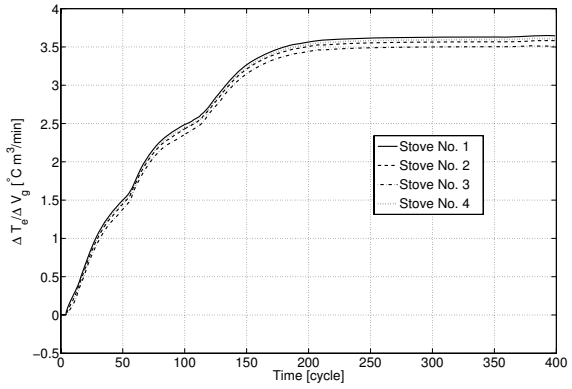

Fig. 4. The response of the end blast temperature deviations from the operating point to a step input in the fourth stove. One cycle lasts for 200 min.

5.2 Disturbance model and estimator

In order to compensate the steady-state offset with MPC algorithms in the presence of unmeasured disturbances or plant-model mismatches, integrating disturbances are introduced in the system model (Muske et al. [2001]). In this work we augment the system state with additional integrating disturbances by the following state disturbance formulation

$$\begin{bmatrix} x(k+1) \\ d(k+1) \end{bmatrix} = \begin{bmatrix} A & B_d \\ 0 & I \end{bmatrix} \begin{bmatrix} x(k) \\ d(k) \end{bmatrix} + \begin{bmatrix} B \\ 0 \end{bmatrix} u(k) + \begin{bmatrix} 0 \\ B_w \end{bmatrix} \omega(k) \tag{7}$$

$$y(k) = [C\ 0] \begin{bmatrix} x(k) \\ d(k) \end{bmatrix} + \nu(k) \tag{8}$$

where $d = \left[d_e^T, d_b^T\right]^T$ is the integrating disturbance with $d_e, d_b \in \mathbb{R}^4$. $w \in \mathbb{R}^{16}$ and $\nu \in \mathbb{R}^8$ are the zero-mean white noise disturbance and output noises respectively with unit covariance matrices. B_d determines the effect of disturbance on the state. There is no general rule for selecting B_d. Here we consider that the disturbance d_e influences the state x_e and the disturbance d_b influences the state x_b through the input channels. Therefore, we chose B_d as

$$B_d = \begin{bmatrix} B_e & 0 \\ 0 & B_b \end{bmatrix}. \tag{9}$$

According to equation (7) the noise w acts only on the integrating disturbance d through the matrix $B_w \in \mathbb{R}^{8\times 8}$ and not on the state x. x and d are estimated from the plant measurement by using a standard time-invariant Kalman filter

$$\begin{bmatrix} \hat{x}(k|k) \\ \hat{d}(k|k) \end{bmatrix} = \begin{bmatrix} \hat{x}(k|k-1) \\ \hat{d}(k|k-1) \end{bmatrix} + \begin{bmatrix} L_x \\ L_d \end{bmatrix} (y(k) - C\hat{x}(k|k-1)) \tag{10}$$

where $L_x \in \mathbb{R}^{8\times 8}$ and $L_d \in \mathbb{R}^{8\times 8}$ are the Kalman filter gain matrices for the state and the integrating disturbances respectively. Since w and ν have unit covariance matrices and considering B_d is fixed, the Kalman filter

gains are adjusted by tuning the matrix B_w. The estimated state $\left[\hat{x}(k|k)^T, \hat{d}(k|k)^T\right]$ is then used in predicting the future augmented state

$$\begin{bmatrix} \hat{x}(k+1|k) \\ \hat{d}(k+1|k) \end{bmatrix} = \begin{bmatrix} A & B_d \\ 0 & I \end{bmatrix} \begin{bmatrix} \hat{x}(k|k) \\ \hat{d}(k|k) \end{bmatrix} + \begin{bmatrix} B \\ 0 \end{bmatrix} u(k). \quad (11)$$

5.3 MPC Formulation

The optimal control problem is formulated in MATLAB using the MPC Toolbox (Bemporad et al. [2004]). The augmented internal model used for predicting the future evolution of the plant can be written as

$$\tilde{x}(k+1) = \tilde{A}\tilde{x}(k) + \tilde{B}u(k) \quad (12)$$

$$y(k) = \tilde{C}\tilde{x}(k) \quad (13)$$

where $\tilde{x} = \left[x^T, d^T\right]^T$ and the matrices $\tilde{A}$, $\tilde{B}$ and $\tilde{C}$ are given in equations (7) and (8) considering w and v are zero.

The lower bounds on the end blast temperature and the brick temperature are modeled as soft constraints with slack variables $\varepsilon_e(k)$ and $\varepsilon_b(k)$ respectively and formulated as

$$y_{e,min} - \varepsilon_e(k) \leq y_e(k), \quad 0 \leq \varepsilon_e(k), \quad (14)$$

$$y_{b,min} - \varepsilon_b(k) \leq y_b(k), \quad 0 \leq \varepsilon_b(k). \quad (15)$$

As mentioned in the problem formulation, the control objective is to drive down the end blast temperature to its constraint value while respecting the constraint on the brick temperature. Therefore, the cost function is formulated as

$$J_N = \min_{\substack{\Delta u(t|t)\ldots\Delta u(t+N-1|t) \\ \varepsilon(t|t)\ldots\varepsilon(t+N-1|t)}} \sum_{k=0}^{N-1} \|y_e(t+k|t) - r\|_{\mathcal{Q}}^2 + \|\Delta u(t+k|t)\|_{\mathcal{R}}^2 + \|\varepsilon(t+k|t)\|_{\mathcal{Q}_\varepsilon}^2 \quad (16)$$

where $r = y_{e,min}$, $\varepsilon = \left[\varepsilon_e^T, \varepsilon_b^T\right]^T$ and $\Delta u(k) = u(k) - u(k-1)$. N is the prediction horizon and $\mathcal{Q}$, $\mathcal{R}$ and $\mathcal{Q}_\varepsilon$ are the nonnegative diagonal weighting matrices. While $\mathcal{Q}$ penalizes the deviation of the output from the set point $\mathcal{R}$ penalizes the input variations. $\mathcal{Q}_\varepsilon$ penalizes the constraint violations and hence its value is chosen to be larger compared to the other weights. The optimal control sequence, $\Delta u(t|t) \ldots \Delta u(t+N-1|t)$, is obtained by minimizing equation (16) subject to the model (12), (13) and the constraints (14), (15).

6. SIMULATION RESULTS

The MPC scheme based on the linear control model is tested on the detailed nonlinear model by simulations. In the detailed model, the on-gas and on-blast phases are chosen to be 100min and hence one period is equal to 50min.

6.1 Steady-state analysis

We first analyze the cost and the constraints of the system at steady-state to investigate the optimal operating point. In Fig. 5 the steady-state values of the end blast temperature and the brick temperature as a function of the exhaust gas flow rate are drawn and the constraints are marked. These values are obtained from simulations with the detailed model. Note that we determined the end blast temperature constraint according to a cold blast mixing flow rate peak that is well above its lower bound. In the real operation this constraint needs to be defined by the operators based on the real operation data and the experiences of the operators. As may be seen in this figure, the constraint on the minimum brick temperature (570°C) is reached when the exhaust gas flow rate is 2308$\mathrm{Nm}^3/\mathrm{min}$. On the other hand, the minimum end blast temperature constraint (1280.5°C) is obtained with 2300$\mathrm{Nm}^3/\mathrm{min}$. Clearly the operation is optimal when the brick temperature is at its constrained value, in other words when the brick temperature constraint is active.

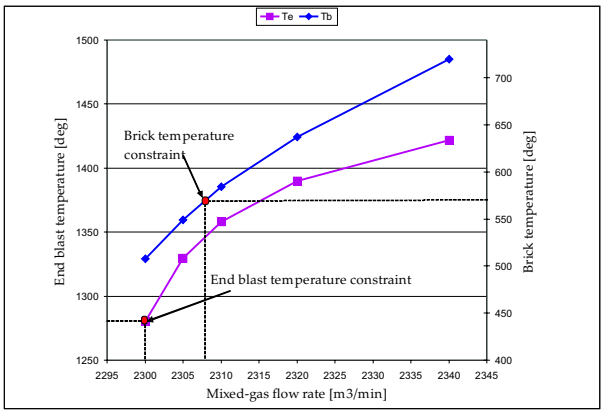

Fig. 5. Steady-state values of the input and outputs obtained with detailed model simulations

6.2 Control performance

The following parameters are used for MPC in simulations: $N = 10$cycles, $\mathcal{Q} = \mathrm{diag}\left([1 \ldots 1]\right)$, $\mathcal{R} = \mathrm{diag}\left([15 \ldots 15]\right)$, $\mathcal{Q}_\varepsilon = \mathrm{diag}\left([10^5 \ldots 10^5]\right)$ and $B_w = \mathrm{diag}\left([10 \ldots 10]\right)$. The MPC scheme is tested with the following scenario: The stoves are initially overheated and they are at the following steady-state operating point: $V_{g,i} = 2340\mathrm{Nm}^3/\mathrm{min}$, $T_{e,i} = 1420°\mathrm{C}$ and $T_{b,i} = 720°\mathrm{C}$ for $(i = 1, 2, 3, 4)$. The control performance is given in Fig. 6. Note that the $x-$ axis of this figure is given in periods unlike the step response plots given in Fig. 4. The variables in $y-$ axis of Fig. 6 are the combinations of the measurements in the four successive periods that form a cycle. For example, the four end blast temperatures at cycle 1 are given at the four successive periods, 1, 2, 3, and 4.

According to Fig. 6 the brick temperature constraint, and hence the optimal operating point is reached in approximately 200 periods (50 cycles), which is four times faster than the open loop response of the system. The brick temperature constraint is violated by at most 2°C. The

reason for this violation is that at the instance of violation the brick temperature estimation error is nonzero. It should also be noted that the optimal operating point and the operating point, where we obtained the linear model are different. Nevertheless, MPC forces the system to the optimal operating point with almost zero steady-state error (0.8°C), which is mainly achieved by the disturbance model we introduced. This is an important advantage of the MPC scheme augmented with the disturbance model, since it allows us to use one model for any operating condition, i.e., we do not have to identify a new model for every new operating condition.

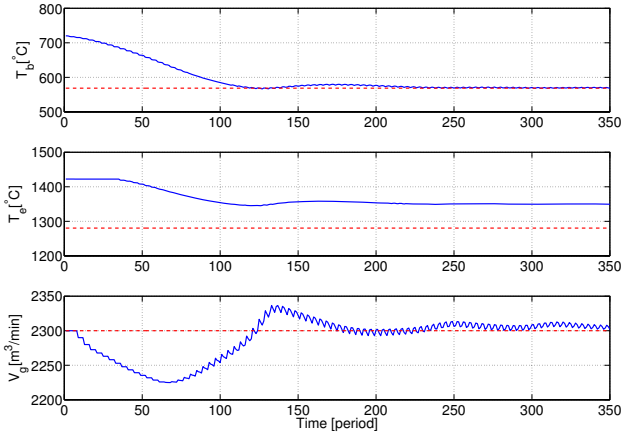

Fig. 6. Control performance of the MPC scheme. *Top figure:* The brick temperature (solid line) and the brick temperature constraint (dashed line). *Middle figure:* The end blast temperature (solid line) and the end blast temperature constraint (dashed line). *Bottom figure:* The control input, exhaust gas gas flow rate (solid line) and the nominal value of the input (dashed line), where the step response experiment is done.

The set of active constraints of a system may change during the operation due to a change in the operating conditions or external disturbances. Since the constraints are incorporated in MPC explicitly, active constraint changes should be handled by MPC. In order to test the performance of the MPC scheme under active constraint changes we modified the end blast temperature constraint for all stoves to ($T_{e,min} = 1370$°C), so that the new active constraint is the end blast temperature constraint. The same MPC parameters of the previous scenario are used. The simulation results are given in Fig. 7. The end blast temperature constraint is reached in 150 periods with negligible offset (0.4°C) and the brick temperature constraint is not violated during the control action. The maximum violation of the end blast temperature constraint is 2°C, which mainly results from the end blast temperature estimation error. From this simulation result, we can conclude that MPC is able to handle the active constraint change during the operation.

7. CONCLUSION

In this paper we presented an optimizing control scheme for the minimization of the energy consumption in the

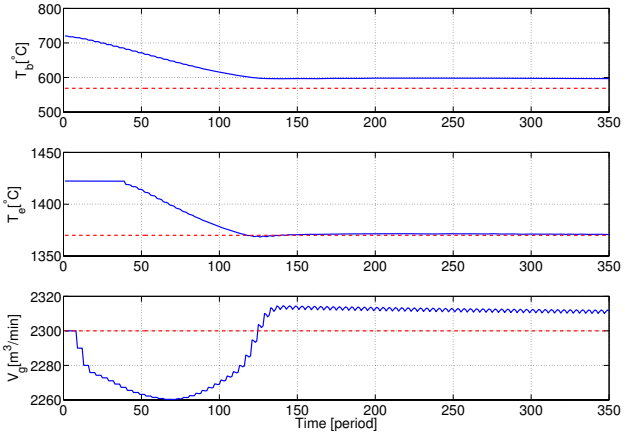

Fig. 7. Control performance of the MPC scheme in case of active constraint change. *Top figure:* The brick temperature (solid line) and the brick temperature constraint (dashed line). *Middle figure:* The end blast temperature (solid line) and the end blast temperature constraint (dashed line). *Bottom figure:* The control input, exhaust gas flow rate (solid line) and the nominal value of the input (dashed line), where the step response experiment is done.

hot blast stoves. The problem of energy minimization in the presence of constraints is formulated as a constrained optimal control problem by selecting an appropriate control structure. A model predictive control scheme, based on a simple linear control model, is designed and implemented on a nonlinear detailed dynamical model. Through simulations it is shown that the MPC scheme performs well under different operating conditions.

REFERENCES

A. Bemporad, M. Morari and N. L. Ricker. *Model Predictive Control Toolbox for Matlab - User's Guide*. Natick, MA: The Mathworks, Inc., 2004.

H. Kwakernaak, P. Tijssen and R. C. W. Strijbos. Optimal operation of blast furnace stoves. *Automatica*, 6:33–40, 1970.

J. M. Maciejowski *Predictive Control*. Prentice Hall, 2002.

Y. Matoba, K. Otsuka, Y. Ueno and M. Onishi. Mathematical model and automatic control system of hot-blast stove. In *Proceedings of the IFAC symposium on Automation in Mining, Mineral and Metal Processing*, , number 10 pages 437–442, 1986.

Kenneth R. Muske, James W. Howse, Glen A. Hansen and Dominic J. Cagliastro. Model-based control of a thermal regenerator. Part 2: control and estimation. *Computers & Chemical Engineering*, 24:2507–2517, March 2000.

Kenneth R. Muske and Thomas A. Badgwell. Disturbance modeling for offset-free linear model predictive control. *Journal of Process Control*, 12:617–632, 2001.

A. J. Willmott. Digital computer simulation of a thermal regenerator. *International Journal of Heat and Mass Transfer*, 7:1291–1302, 1964.

P. Zuidema. Non-stationary operation of a staggered parallel system of blast furnace stoves. *International Journal of Heat and Mass Transfer*, 15: 433–442, 1972.